

IV. RESULTS AND DISCUSSION

A. Computerized Research Facility

1) X-Ray Diffraction System

The computerization of the Norelco XRG 3000 x-ray powder diffraction unit resulted in an efficient tool with which qualitative and quantitative x-ray diffraction could be performed. This unit can be operated in two modes. The first measuring the number of x-ray photons diffracted at a specific 2θ angle over a specific time period which can be selected from 0.1 to 8000 seconds. In the second mode the length of time required to count a chosen number of photons diffracted at a specific angle is measured. Because the standard deviation varies in proportion to the square root of the number of photons counted, the second analysis method is preferred for it maintains a constant standard deviation throughout the collected data set. The lower intensity diffraction peaks are better resolved in the second method for at decreased intensity the system measures longer to count the specified number of photons. The disadvantage of this method is that the system spends considerable time counting at 2θ angles where no diffraction

peaks occur. If a rapid scan is desired which shows the location and intensity of the major diffraction lines, the first method is preferred.

The angle-mode programmer can be programmed to scan from 0 to 90 degrees 2θ or up to 50 separate intervals of this range. The $\Delta 2\theta$ step size can be set from 0.01 degrees 2θ to 0.5 degrees 2θ . The angle mode programmer can be programmed to analyze from 1 to 35 slides which are automatically inserted into the x-ray beam by the automatic sample changer. Software resident in the PDP-20 and LSI 11/23 computers collects the intensity 2θ tuples and stores them in a separate data file for each sample which are labelled FOR10.DAT, FOR11.DAT ... FOR45.DAT. The advantage of storing the diffraction results for each sample in a separate data file is that each file is closed immediately following the collection of the data. Therefore, if the carrier is lost the data from all samples analyzed up to the time of malfunction is protected.

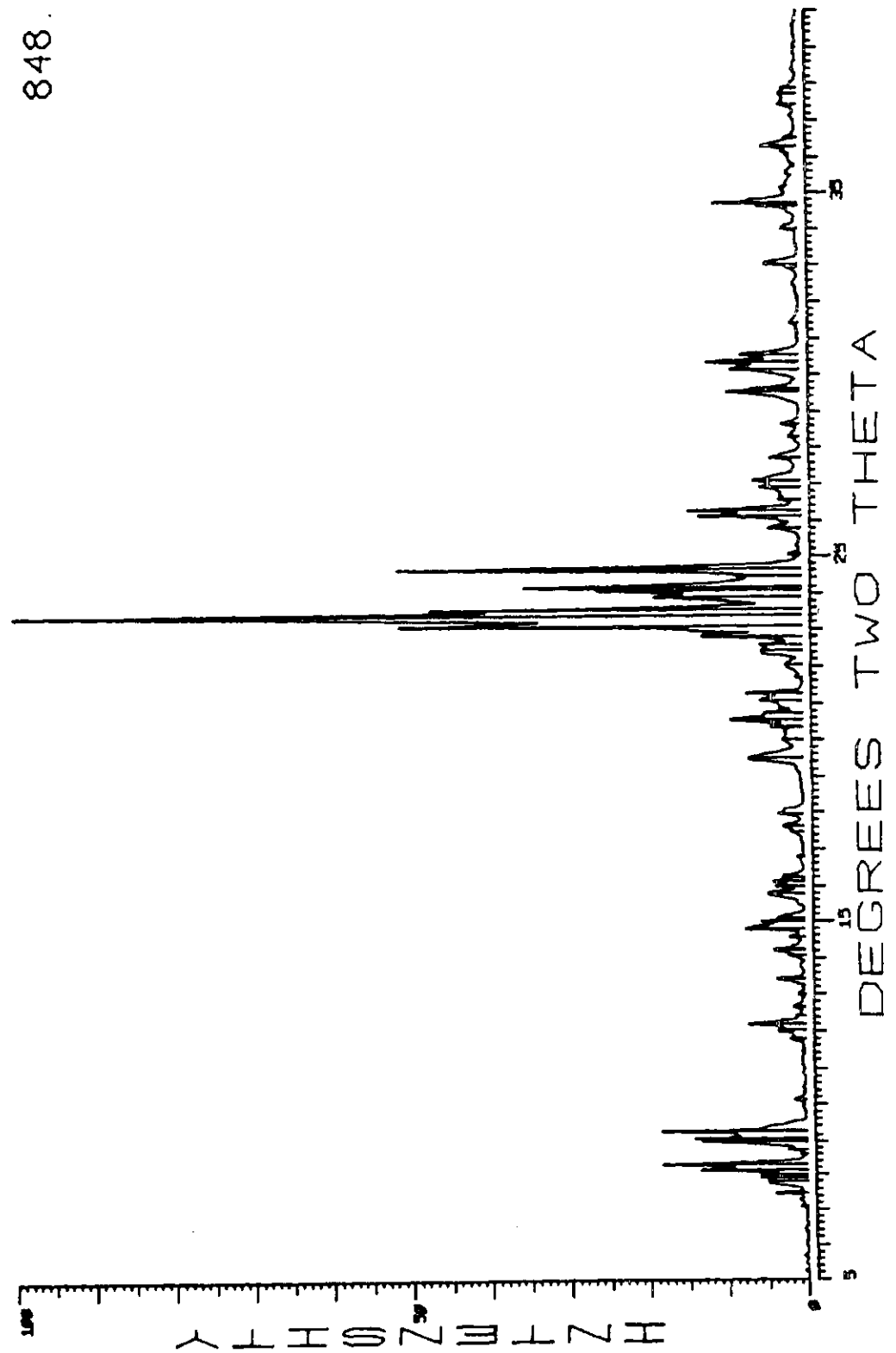
To provide graphic output of the x-ray diffraction patterns, two graphics packages were assembled. The first of these graphics packages was donated by Tektronix Instruments, Inc. to the Department of Chemical Engineering. This Fortran based graphics system was installed on the PDP-20. Because it required approximately 24 K of memory to execute, it was inappropriately large for use on the LSI-11/23 minicomputer. For this reason and because both the Cahn Balance system and Micropilot Plant reactor system also required graphical output of data resident in

the LSI-11/23, a small efficient Macro 11 Assembly language graphics package was written. A listing of this assembly package is provided in Appendix A. Because subsequent operators of this system are unlikely to be familiar with Assembly language programming, all higher level subroutines contained in this graphics package were made callable from Fortran programs. These higher level routines can be called from and linked with very basic Fortran language programs. The graphics package provides for fully automatic scaling of thesis dimension plots including the alpha-numeric labelling of the axis and engineering notation adjustment of the numerical range of each axis. Only five subroutine calls are required to generate a thesis dimension plot. A call to subroutine AXIS contains six arguments necessary to automatically scale the axis. The Fortran command is of the form `CALL AXIS (XMIN, XMAX, YMIN, YMAX, XDIG, YDIG)`. The arguments XMIN and XMAX, are the minimum and maximum real number values to be plotted. Similarly YMIN and YMAX are the actual minimum Y and maximum Y values to be plotted. XDIG and YDIG describe the number of digits to be used in labelling the axis. For instance, if the range of the ordinate was from 4 million to 9 million it would be inappropriate to label the axis 4,000,000, 5,000,000 ... 9,000,00. Instead, if the operator defined YDIG to be the number 1, the axis would be labelled 4, 5, 9 and the operator could use the alpha numeric label to then indicate that the values expressed were "counts x 10⁶". To effect

the alpha numeric labelling of the axis, two subroutine calls are made each containing two arguments. The Fortran language commands are CALL Y AXIS (ARG1, 'YLABEL') and CALL X AXIS (ARG2, 'XLABEL'). In these two subroutine calls ARG1 and ARG2 are the number of alphanumeric characters including spaces contained in the axis labels, Y LABEL and X LABEL, respectively. Once these three subroutine calls are made, the computer automatically draws the cartesian axis, labels them numerically, and draws the titles for each axis. The actual size of the letters in each title are swollen or shrunk depending on the total number of letters used in the label description. The overall dimensions of the plot are, therefore, adjusted to maintain thesis dimensions. The only other subroutine calls which are necessary are calls to MOVEA and DRAWA of the form CALL MOVEA (X,Y) and CALL DRAWA (X,Y). A call to MOVEA causes the pen to lift on the 4662 interactive digital plotter and move to the user coordinate system position X,Y defined in the arguments. A call to DRAWA causes the pen to drop in its present position and draw a line to position X,Y defined in the arguments. Calls to MOVEA and DRAWA can be repeated until the graph is finished. Graphs of any size can also be produced by this graphics system up to 12 inches by 14 inches but for these, the operator must write assembly language calls to the appropriate Macro 11 subroutines shown in Appendix A. A cartesian plot prepared by this 2-dimensional graphics system of the x-ray diffraction data

for ZSM-5 is shown in Figure 57. The background noise in this data set was removed by a program called BRAIN5.REL which is resident on the PDP-20. In powder diffraction data the background noise increases in the low angle 2θ region. This causes a non-linear baseline which increases linear baseline which increases rapidly below 7 degrees 2θ and gradually from 90 to 7 degrees 2θ . To remove this background noise and linearize the baseline, the algorithm begins by subtracting a single photon from the number of counts measured at every 2θ increment. It then checks to see if the intensity value at any 2θ location has become 0. If say, at 36.02 degrees 2θ it finds a 0 intensity value, it then subtracts a photon from the intensity measurements at every 2θ location from the minimum 2θ angle to 35.01 degrees. It again checks for a 0 intensity value at all 2θ locations below 35.01 degrees inclusive. If it finds no 0 intensity value it subtracts a second photon from each of the intensity values mentioned. Eventually, a 0 intensity value occurs at for instance, 22.11 degrees. It then continues this procedure subtracting a photon from the minimum 2θ angle to 22.10. Eventually, the algorithm terminates as the region from which photons are removed, decreases toward the low angles. This procedure works well at flattening the baseline without altering the relative intensity of the diffraction lines above baseline. Once the background noise has been removed,

Figure 57. Cartesian Plot Prepared by
2-dimensional Graphics System
of the X-ray Diffraction Data
For ZSM-5.



the algorithm takes the first derivative of the diffraction data resulting in the information shown in Figure 58. Figure 58 is the first derivative of a ZSM-5 diffraction pattern. The algorithm then looks for regions in which the first derivative data has a decreasing slope. An amplified (5X) plot of this first derivative is shown in Figure 59. The positions at which the decreasing slope of the first derivative cross 0 the intensity maximum of the diffraction peaks are found. The algorithm then uses linear regression to determine the exact 2θ angle at which the peak maximum occurred. The algorithm then uses Bragg's Law to determine the d -spacing of the molecular planes which caused each diffraction line. This information is output in tabular form showing the peak number, the 2θ angle, the d -spacing, and the background corrected intensity. The data can also be output in the form of a diffraction line pattern. Figure 57 shows the diffraction line pattern superimposed on the background corrected diffraction plot. It can be observed that this algorithm not only found every significant diffraction line but also the correct position of each line.

A line pattern can also be generated from intensity, d -spacing information from the powder diffraction index. Using DATFILL.REL to enter the intensity, d -spacing tuples programs LINE.REL and LINE2.REL can be used to prepare literature line patterns over the angles 5 to 40 and 0 to 90 degrees 2θ , respectively. As the physical dimensions

Figure 58. Algorithm Takes First
Derivative of Diffraction
Data - After Background Noise
Removed.

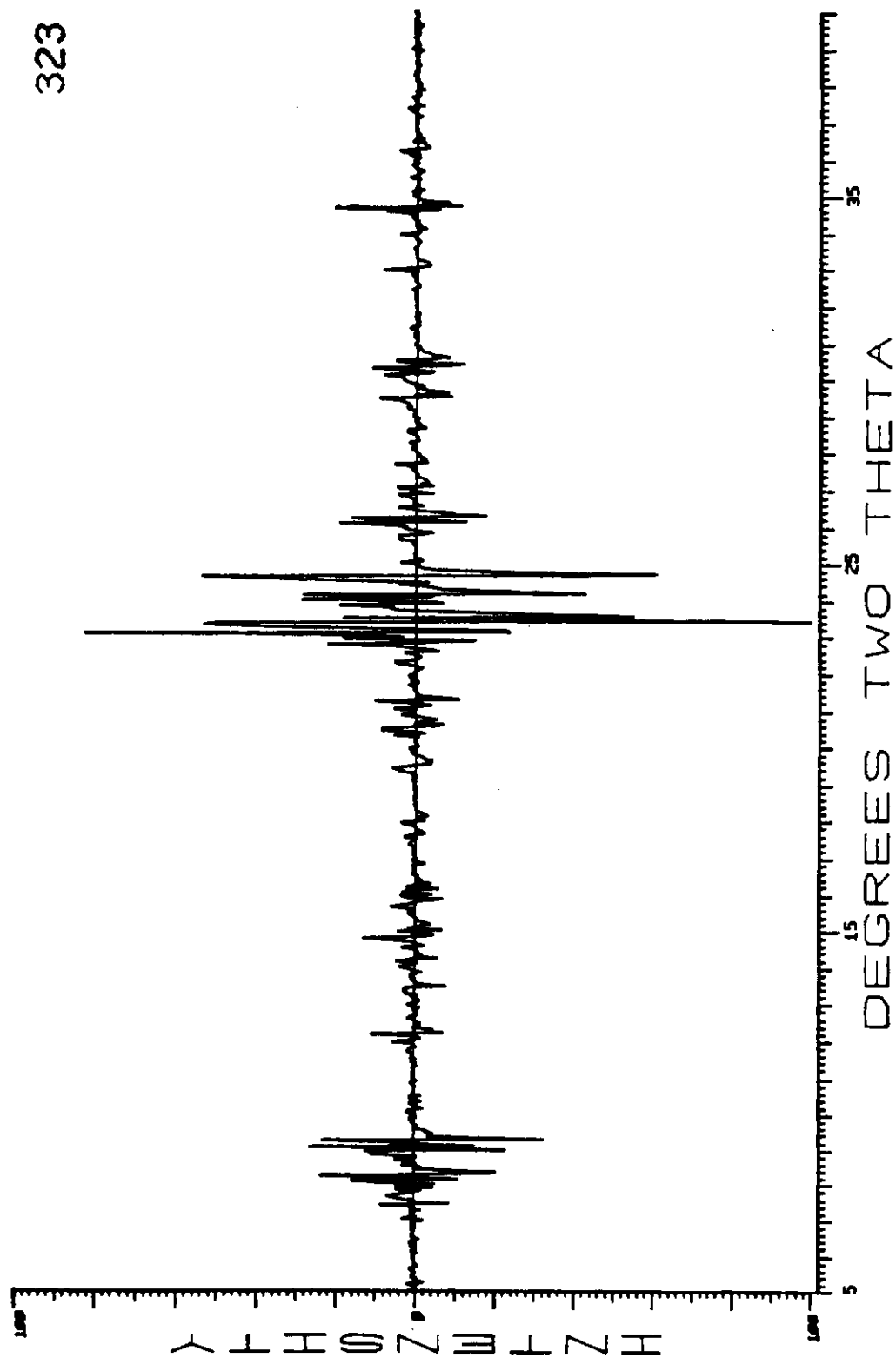
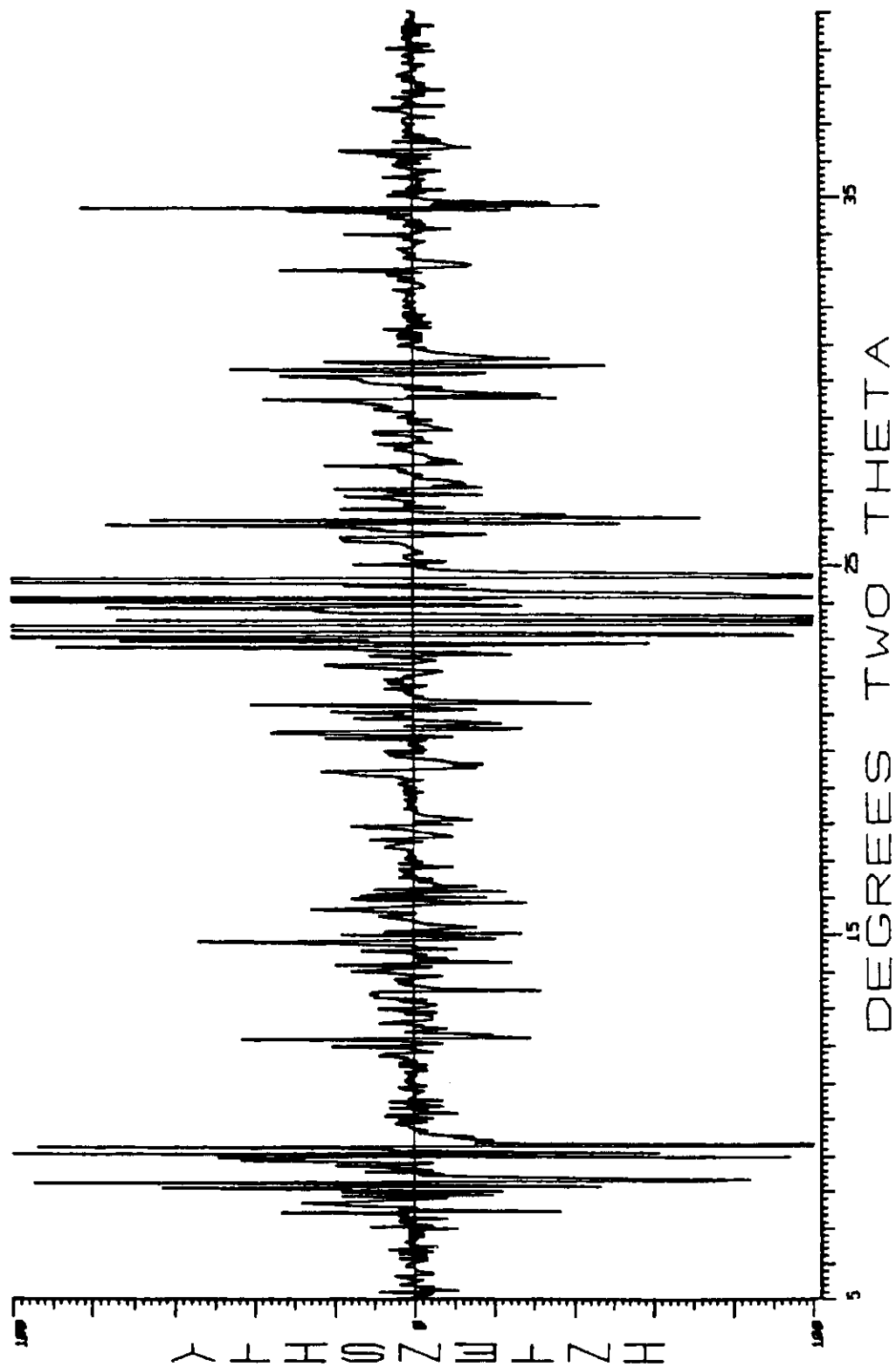
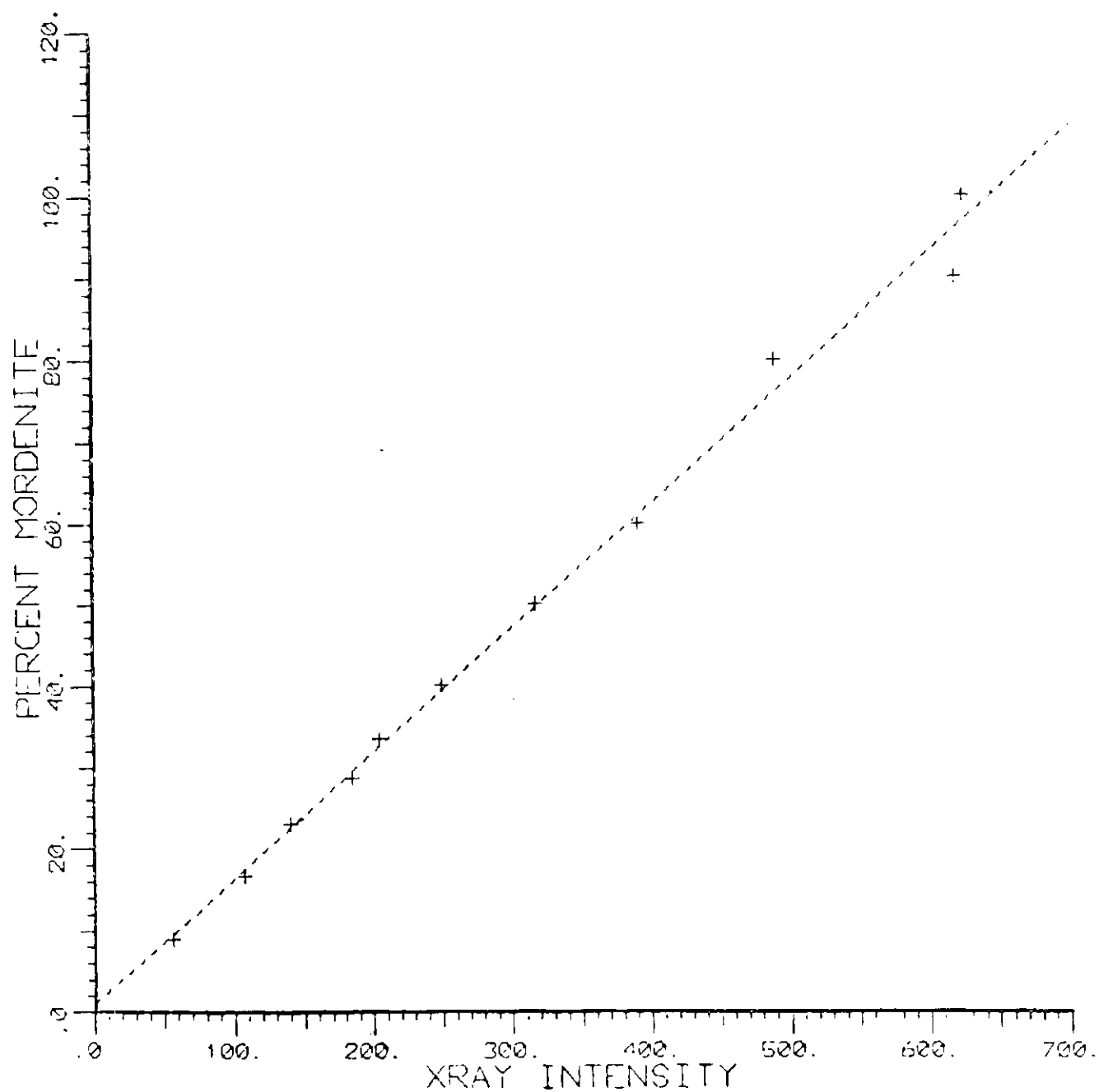


Figure 59. Amplified (5X) Plot of
First Derivative



of the line patterns are equivalent to those of the x-ray diffractogram, the lines attributable to each phase in the sample can be rapidly checked off by placing the literature line pattern behind the diffraction pattern and holding it up to a light. For quantitative analysis a program, ANALYS.FOR, was prepared. To use this program the operator inputs the 2 theta location for 6 diffraction lines. The algorithm sums the background corrected intensity of the 6 chosen lines and reports a total intensity value as its output. A calibration curve must be generated to convert this summed intensity value to phase concentration. The calibration curve is generated by mixing various amounts of an appropriate amorphous material with a pure crystalline phase. An example calibration curve is shown in Figure 60 wherein 5%, 10%, ...95%, 100% of pure crystalline mordenite was mixed with amorphous silica-alumina gel having an equivalent silica to alumina ratio. Each sample was x-rayed and its background corrected data used to produce the summed intensity values outlined. The linear regression fit was good having an R value of 0.95. Using this intensity concentration relationship, the concentration of this phase in an unknown can be predicted from the summed intensity values.

MORDENITE CALIBRATION CURVE



CURVE APPROXIMATION BY
POLYNOMIAL REGRESSION OF DEGREE 1

Figure 60. Calibration Curve

2) Cahn Balance System

The rate at which molecules can diffuse into the intracrystalline pores of zeolite catalysts is an important parameter, for it determines the rate at which acid catalysis can occur on the Bronsted Lewis sites lining the pore system. The measurement of diffusion rates particularly for small molecules is a complex analytical problem, for the introduction of sorbate causes a pressure surge in the balance chamber. The downward force of the sorbate wind on the balance pan causes erroneously high sorption rate measurements for the initial 10 to 15 seconds of the adsorption. For small molecules such as water 80% of the sorption capacity is often reached during the first 30 seconds and perhaps 50% in the first 10 seconds. Modeling the sorption rate becomes difficult for small molecules because the most important portion of the sorption rate curve is destroyed by the sorbate wind, buoyancy and other effects. For bifunctional catalysts the rate of diffusion of small molecules such as hydrogen, carbon monoxide, water, methane, and dimethyl ether is of greatest concern. If metals are incorporated within the pore system of ZSM-5 the reduction in pore diameter they cause at various metal loadings, and their effect on the sorption rates of reactant molecules (and product molecules as well) is critical. To evaluate these sorption rates a fully

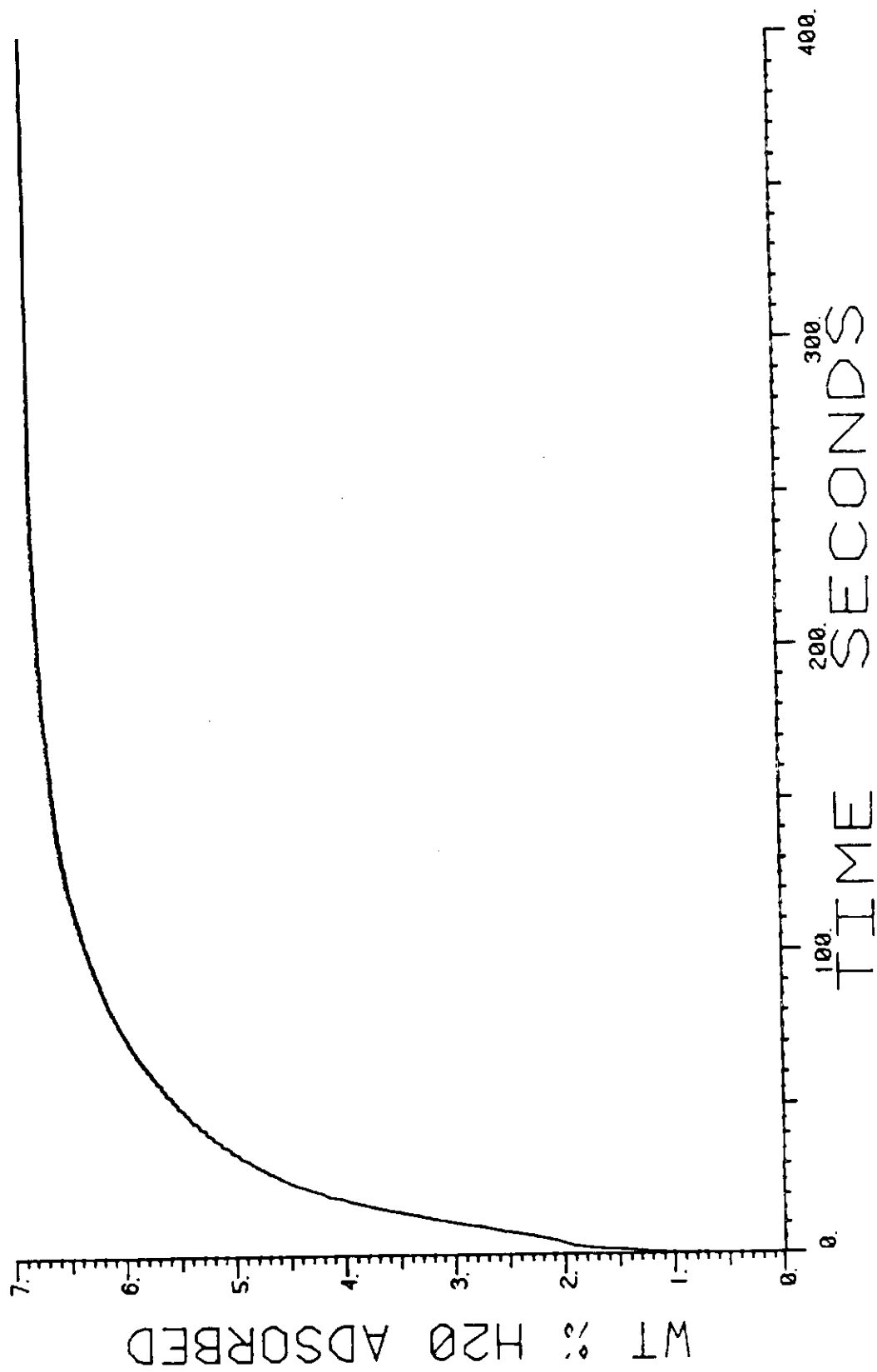
computerized Cahn Balance system was developed. A listing of the Macro 11 program and Fortran program which control the data acquisition from the Cahn Balance system is shown in Appendix B. A typical program used in conjunction with the 2-dimensional Macro 11 plotting package (see x-ray section and Appendix A) is also listed in Appendix B. A method was devised through which the effect of the sorbate pressure surge and buoyancy could be removed from the data set such that accurate diffusion rates could be determined for small molecules. In accordance with the procedure outlined in Section III B.2. and under the control of the program listed in Appendix B, the sorption rate data are obtained at the rate of 50 observations per second at the rated accuracy of the Cahn Balance. The rate data is transferred from the floppy disc to the Winchester disc to preserve a copy. The identical experiment i.e., same sorbate, same pressure is then carried out on a non-adsorbing blank. This data set shows a substantial peak centered typically at 8 seconds which is caused by the force induced by the sorbate wind on the balance pan. When this data set is subtracted from the data set accumulated on the zeolite sample, the difference represents a considerably more accurate statement of the true sorption rate curve. If oscillations are still present, the sorption rate data can be transformed into frequency space using a DEC algorithm resident on the LSI-11/23 which performs the discrete fast Fourier transform. In frequency space, noise caused by the harmonic oscillation of the Balance

arm is centered at approximately 6 per minute. Deleting the real and complex Fourier co-efficients of these noise harmonics followed by the application of the inverse transform presents the data back in time space. Subtracting the filtered data set from its precursor results in a data set describing a sine wave which should be centered at 0 and horizontal. An example of the product of this digitally filtered rate curve is shown in Figure 61. This rate curve was produced at ambient temperature at 4 mm H₂O vapor pressure on ZSM-5 having a 40:1 silica to alumina ratio. An additional advantage of collecting sorption rate curves digitally over the traditional analog method, is that an nth order polynomial regression fit can be performed on the multitude of data points collected. The polynomial regression fit enables the specific shape of the rate curve to be stored for future use in as few as 5 constants. The procedure utilized by the regression algorithm is defined as follows.

Selecting the specific case where we wish to employ a 4th order polynomial regression fit of the set of weight, (time)^{1/2} tuples, we therefore desire the polynomial of the form $Y = A + BX + CX^2 + DX^3 + EX^4$ which, to the extent possible, follows the course of the measured data.

Optimally: $O = A + BX + CX^2 + DX^3 + EX^4$. However, some deviation will exist which we will label D. Therefore: $D = A + BX + CX^2 + DX^3 + EX^4$. In taking the sum of the deviations over the available data points we do not want positive and negative deviations to cancel each other and

Figure 61. Digitally Filtered Rate Curve



and we will therefore square both sides

$$\sum_{1}^N d^2 = \sum_{1}^N (A + BX + CX^2 + DX^3 + EX^4)^2$$

In this function $F(A, B, C, D, E)$ we wish to select constants A, B, C, D, E , such that this function (the sum of the square of the deviation) is minimized. We therefore take the partial derivative of the error function with respect to each variable and set it equal to zero.

Thus

$$\begin{aligned} 1) \quad \frac{\delta F}{\delta A} &= \sum \frac{\delta}{\delta A} (A + BX + CX^2 + DX^3 + EX^4 - Y)^2 \\ &= \sum 2X (A + BX + CX^2 + DX^3 + EX^4 - Y) \end{aligned}$$

$$\begin{aligned} 2) \quad \frac{\delta F}{\delta B} &= \sum \frac{\delta}{\delta B} (A + BX + CX^2 + DX^3 + EX^4 - Y)^2 \\ &= \sum 2X (A + BX + CX^2 + DX^3 + EX^4 - Y) \end{aligned}$$

$$\begin{aligned} 3) \quad \frac{\delta F}{\delta C} &= \frac{\delta}{\delta C} (A + BX + CX^2 + DX^3 + EX^4 - Y)^2 \\ &= \sum 2X^2 (A + BX + CX^2 + DX^3 + EX^4 - Y) \end{aligned}$$

$$4) \quad \frac{\delta F}{\delta D} = \sum \frac{\delta}{\delta D} (A + B + CX^2 + DX^3 + EX^4 - Y)^2$$

$$= \sum 2X^3 (A + BX + CX^2 + DX^3 + EX^4 - Y)$$

$$5) \quad \frac{\delta F}{\delta E} = \frac{\delta}{\delta E} (A + BX + CX^2 + DX^3 + EX^4 - Y)^2$$

$$= \sum 2X^4 (A + BX + CX^2 + DX^3 + EX^4 - Y)$$

These equations (1-5) can be easily reduced to the following

$$6) \quad \sum Y = nA + B\sum X + C\sum X^2 + D\sum X^3 + E\sum X^4$$

$$7) \quad \sum XY = A\sum X + B\sum X^2 + C\sum X^3 + D\sum X^4 + E\sum X^5$$

$$8) \quad \sum X^2 Y = A\sum X^2 + B\sum X^3 + C\sum X^4 + D\sum X^5 + E\sum X^6$$

$$9) \quad \sum X^3 Y = A\sum X^3 + B\sum X^4 + C\sum X^5 + D\sum X^6 + E\sum X^7$$

$$10) \quad \sum X^4 Y = A\sum X^4 + B\sum X^5 + C\sum X^6 + D\sum X^7 + E\sum X^8$$

To solve these simultaneous equations in the general case, we will represent them as a 5x5 matrix

$$\begin{bmatrix} n & \sum X & \sum X^2 & \sum X^3 & \sum X^4 \\ \sum X & \sum X^2 & \sum X^3 & \sum X^4 & \sum X^5 \\ \sum X^2 & \sum X^3 & \sum X^4 & \sum X^5 & \sum X^6 \\ \sum X^3 & \sum X^4 & \sum X^5 & \sum X^6 & \sum X^7 \\ \sum X^4 & \sum X^5 & \sum X^6 & \sum X^7 & \sum X^8 \end{bmatrix} \begin{bmatrix} A \\ B \\ C \\ D \\ E \end{bmatrix} = \begin{bmatrix} \sum Y \\ \sum XY \\ \sum X^2 Y \\ \sum X^3 Y \\ \sum X^4 Y \end{bmatrix}$$

Evaluating the summation terms in the 5X5 matrix for a specific data set, applying a matrix inversion subroutine written by Digital provides the solution through the multiplication of both sides by the inverse.

$$\begin{bmatrix} 1 \\ 1 \\ 1 \\ 1 \\ 1 \end{bmatrix} \begin{bmatrix} A \\ B \\ C \\ D \\ E \end{bmatrix} = \begin{bmatrix} \sum X \\ \sum XY \\ \sum X^2 Y \\ \sum X^3 Y \\ \sum X^4 Y \end{bmatrix} \begin{bmatrix} n & \sum X & \sum X^2 & \sum X^3 & \sum X^4 \\ \sum X & \sum X^2 & \sum X^3 & \sum X^4 & \sum X^5 \\ \sum X^2 & \sum X^3 & \sum X^4 & \sum X^5 & \sum X^6 \\ \sum X^3 & \sum X^4 & \sum X^5 & \sum X^6 & \sum X^7 \\ \sum X^4 & \sum X^5 & \sum X^6 & \sum X^7 & \sum X^8 \end{bmatrix}^{-1}$$

The model of Crank¹⁶⁹ describing the non-steady state diffusion in a sphere at constant surface concentration is often used to model zeolite diffusivity. Crank's solution describing the total amount of a diffusing substance entering or leaving a sphere is given by:

$$\frac{M_t}{M_\infty} = 1 - \frac{6}{\pi^2} \sum_{n=1}^{\infty} \frac{1}{n^2} \exp(-D_n \pi^2 t/a^2)$$

The diffusivity D can be evaluated recursively to obtain the best fit with the regression model. Plotting the actual rate data against the square root of time instead of time enables a direct linear regression fit as shown in Figure 62. When this approach was used on the sorption data for 2 mm normal heptane on ZSM-5, the correlation coefficient was excellent ($R=0.9944$). The slope was determined to be 1.411 and the intercept -0.4897. The linearity of wt.% octane adsorbed when plotted against square root of time was even more apparent as is shown in Figure 63. This system was used to screen all catalysts before reactor studies were made. If the zeolite pores were blocked during the synthesis, calcination, or metal impregnation steps there was little to be gained from wasting costly reactor time on such inactive catalysts.

The selectivity cross over for ZSM-5 catalysts of varying silica to alumina ratio was evaluated. As can be seen in Table 25 there is a strong tendency for ZSM-5 to become increasingly hydrophobic and organophillic with increasing silica

Figure 62. Direct Linear Regression Fit

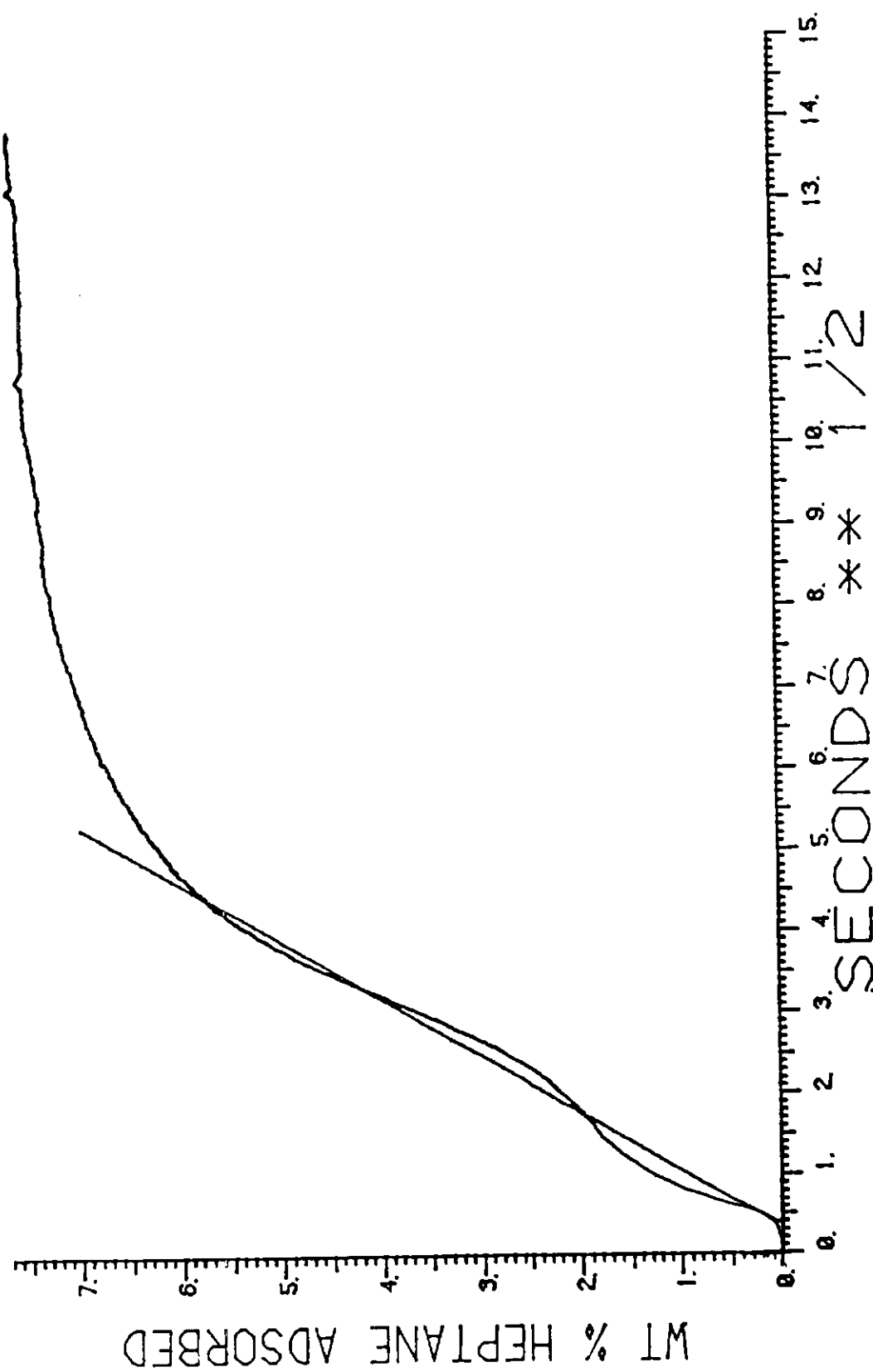


Figure 63. Linearity of wt.% octane

Adsorbed when plotted

against square root of time

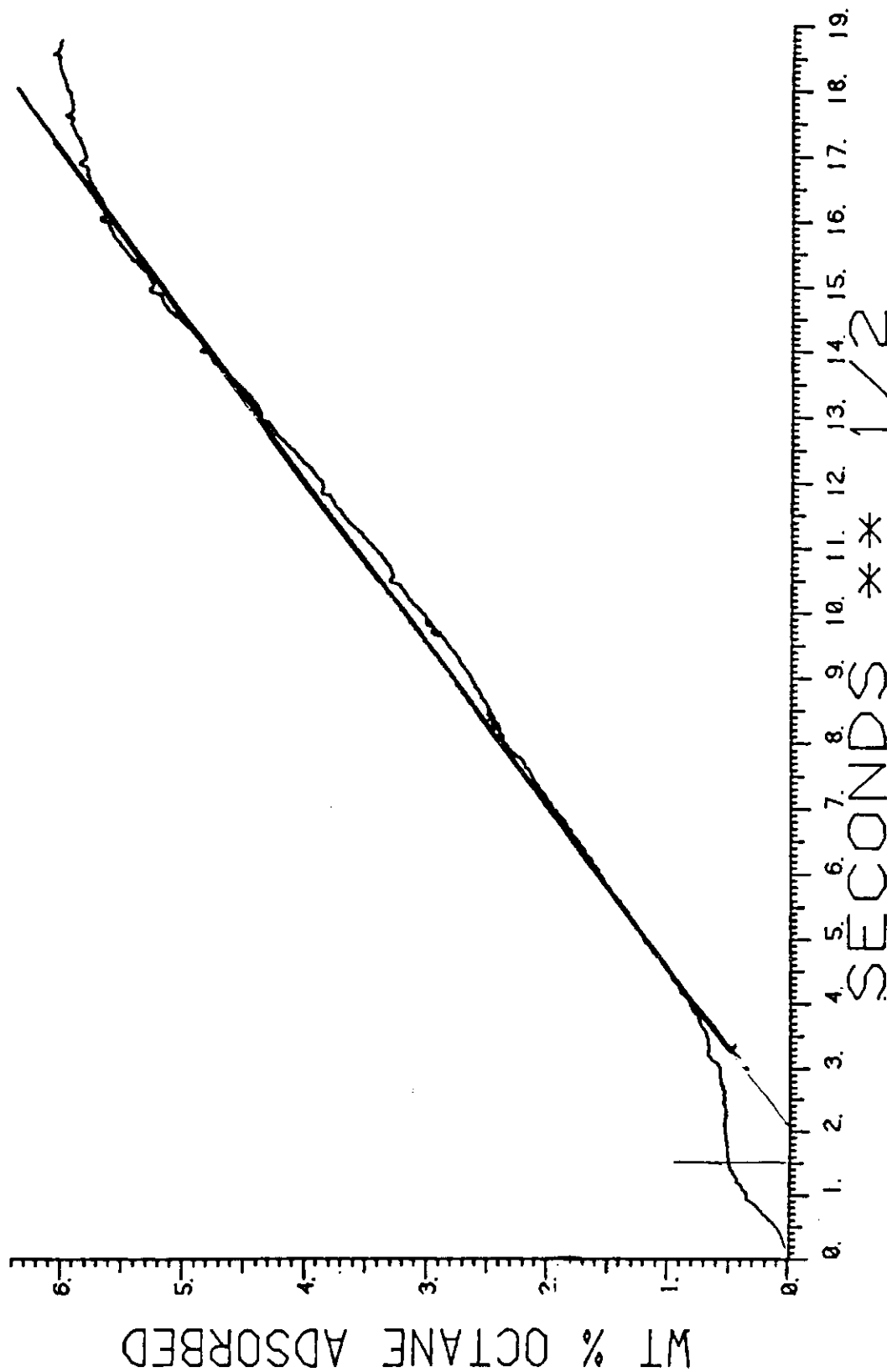


Table 25. Near-Equilibrium Adsorption capacities
(g/100g) for ZSM-5 Synthesized with
Varying $\text{SiO}_2/\text{Al}_2\text{O}_3$ Ratios.

$\text{SiO}_2/\text{Al}_2\text{O}_3$	24 min., 6.5 Torr		% Crystallinity
	H_2O	n-Hexane	by XRD
30/1	8.8	5.0	51
40/1	6.3	8.4	63
50/1	4.7	10.2	70
60/1	3.4	9.2	82

to alumina ratio. When the aluminum content was highest (i.e., 30:1 silica to alumina) the lattice was most polar and the largest amount of water adsorbed i.e., 8.8 wt.%. To plot the effect of temperature or pressure on sorption rate curves or other 3-dimensional graphs such as crystal structures, a 3-dimensional graphics system was prepared in Fortran. A listing of this 3-dimensional graphics package and thorough description of its subroutines is provided in Appendix C.